Bulk Edge Correspondence to Chevron-type Graphene Nanoribbons

Chih-Yu Hsu
Dr. Mei-Yin Chou
NTU PHYS/IAMS

Sep. 13, 2017

Outline

Introduction

- "We show that semiconducting graphene nanoribbons (GNRs) of different width, edge, and end termination belong to different electronic topological classes."

Termination type	Zigzag (N = Odd)	Zigzag' (N = Odd)	Zigzag (N = Even)	Bearded (N = Even)
Unit cell shape	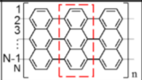	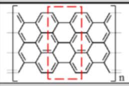	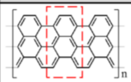	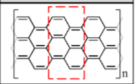
Bulk Symmetry	Inversion/mirror	Inversion/mirror	Mirror	Inversion
Z_2	$\frac{1+(-1)^{\lfloor\frac{N}{3}\rfloor+\lfloor\frac{N+1}{2}\rfloor}}{2}$	$\frac{1-(-1)^{\lfloor\frac{N}{3}\rfloor+\lfloor\frac{N+1}{2}\rfloor}}{2}$		$\frac{1-(-1)^{\lfloor\frac{N}{3}\rfloor}}{2}$

Ting Cao, Fangzhou Zhao, and Steven G. Louie, Phys. Rev. Lett. 119, 076401 (2017).

Graphene Nanoribbons

- Graphene: 2-dim
- Graphene Nanoribbons (GNRs): 1-dim
- Armchair GNRs
- Zigzag GNRs

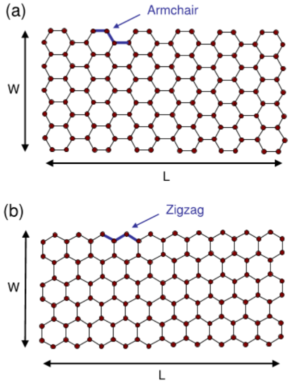

Ragheb T, Massoud Y, IEEE/ACM Int. Conf. on Computer-Aided Design p.593 (2008).

GNRs Produced in Labs Recently

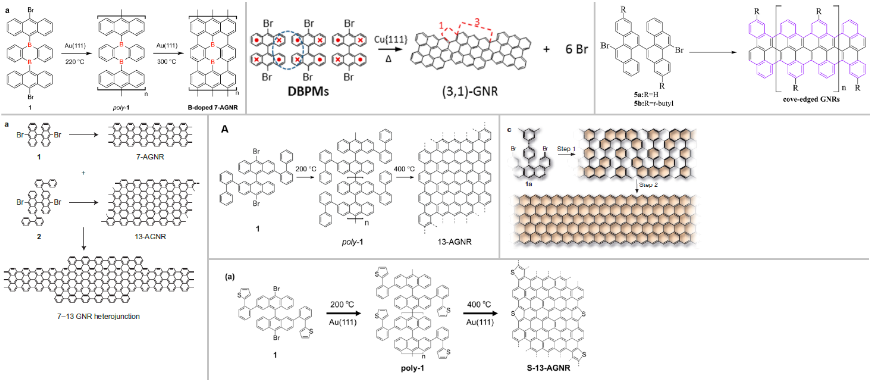

J. Am. Chem. Soc., 137 (28), pp 8872–8875 (2015). ACS Nano, 8 (9), pp 9181–9187 (2014). J. Am. Chem. Soc., 137 (18), pp 6097–6103 (2015). Nature Nanotechnology 10, 156–160 (2015). ACS Nano, 2013, 7 (7), pp 6123–6128. Nature 531, 489–492 (2016). J. Phys. Chem. C, 120 (5), pp 2684–2687 (2016).

AGNR Band Structure

- Tight-binding model
- $E = \pm t|2e^{-ik_x a/2} \cos\left(\frac{\sqrt{3}a}{2} q_y\right) + e^{ik_x a}|$
- $q_y = \frac{2}{\sqrt{3}a} \frac{p\pi}{N+1}$
- Valence band v.s. Conduction band

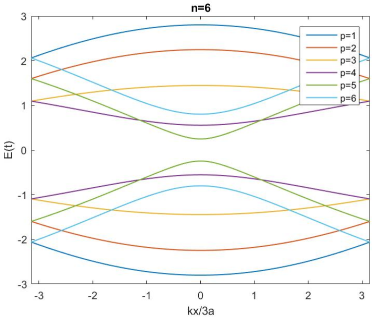

AGNR Band Structure: Flat Band

- $p = 4$
  $\rightarrow \cos \frac{p\pi}{N+1} = \cos \frac{\pi}{2} = 0$
  $\rightarrow$ flat valence or conduction band
- Energy dispersion: independent of k_x
- Eigenenergy$= \pm t$
- A flat band exists only when N is odd.

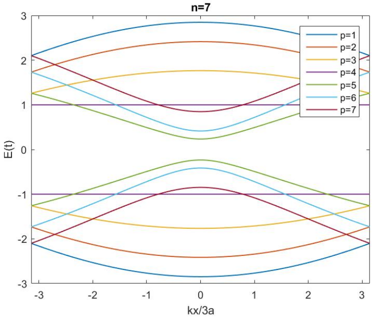

AGNR Band Structure: Energy Gap=0

- $k_x = 0$
  $\rightarrow E = \pm t|2\cos\frac{p\pi}{N+1} + 1|$
- $N = 3m + 2, p = 2m + 2$
  $\rightarrow \frac{p\pi}{N+1} = \frac{2\pi}{3}$
  $\rightarrow E = 0$
  $\rightarrow$ Energy gap$= 0$

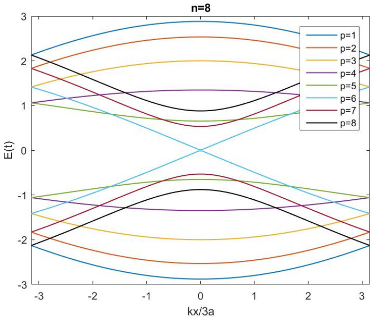

ZGNR Band Structure

- AGNR BC
  $\phi_A(0) = \phi_A(N+1) = 0$
  $\phi_B(0) = \phi_B(N+1) = 0$
- ZGNR BC
  $\phi_B(0) = 0$
  $\phi_A(N+1) = 0$

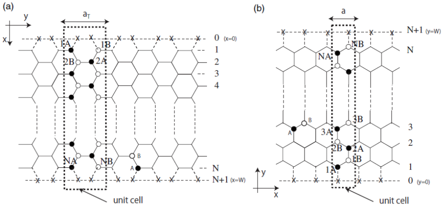

  - Armchair graphene nanoribbons
    $E = \pm\left|2e^{-ik_x a/2}\cos\left(\frac{\sqrt{3}a}{2}q_y\right) + e^{ik_x a}\right|$
  - Zigzag graphene nanoribbons
    $E = \pm\sqrt{1 + g_k^2 + 2g_k\cos p}$
    $F(p, N) \equiv \sin(pN) + g_k\sin(p(N+1)) = 0$

K. Wakabayashi, K. Sasaki, T. Nakanishi, and T. Enoki, Sci. Technol. Adv. Mater. 11, 054504 (2010).

ZGNR Band Structure

- The 2 solutions are different due to different BCs.
- The electronic states in flat bands, $\frac{2}{3}\pi \leq |k| \leq \pi$, corresponds to a state localized on the edge sites. (Edge state)

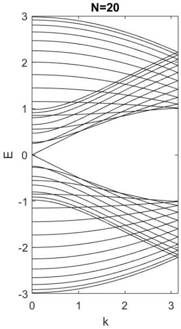

Figure 1: AGNR

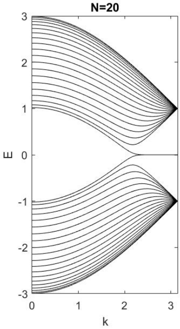

Figure 2: ZGNR

ZGNR Edge State

- Edge state $\in$ Surface state
- Semi-infinite graphene sheet
  Flat band: $\frac{2}{3}\pi \le |k| \le \pi$
- Real part of wave function
  Amplitude $\propto$ Radius / Color : $\pm$
- $k = \pi$: localized at edge sites
  $k = \frac{2}{3}\pi$: penetrated into inner sites

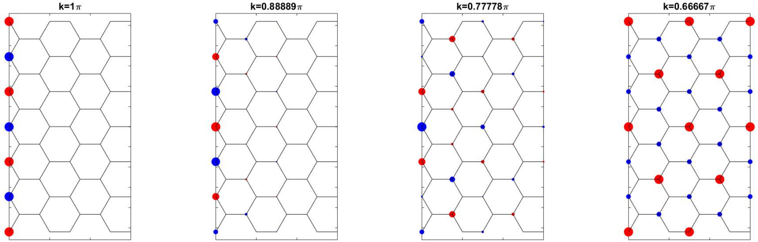

Zak Phase and Parity

- Berry phase: geometric phase
  $\gamma = i \oint_c \langle n, t | \nabla_R | n, t \rangle \, dR$
- 1-dim Brilloiun zone $\rightarrow$ circle
- Zak phase: Berry phase in solid state
  $Z = i \int_{-\pi}^{\pi} \langle u_{nk} | \partial_k | u_{nk} \rangle \, dk$
- Zak phase = intercell part (indep. of origin) + intracell part
  Origin of the unit cell = Inversion or mirror center
  $\rightarrow$ Zak phase = intercell part
- An easier way to compute Zak phase is by computing parity.
- $(-1)^{Z_2} = e^{i \sum\limits_n \gamma_n^{inter}} = \prod\limits_{k=0,\pi} \delta(k)$
  $\delta(k) = \prod\limits_{n \in occupied} \xi_n(k)$
- Zak phase: bulk property

Prediction of n_s

- n_s:number of in-gap surface states below Fermi level
- $n_s = \frac{\sum_{n \in occupied} \gamma_n^{inter}}{\pi} \text{mod } 2$
- For systems with inversion symmetry,
  $Z_2 = (n_0^{I,-} + n_\pi^{I,-}) \text{ mod } 2 = 0$
  $\rightarrow n_s \text{ mod } 2 = 0$
  $Z_2 = (n_0^{I,-} + n_\pi^{I,-}) \text{ mod } 2 = 1$
  $\rightarrow n_s \text{ mod } 2 = 1$
- For systems with mirror symmetry,
  $Z_2 = (n_0^{M,-} + n_\pi^{M,-}) \text{ mod } 2 = 0$
  $\rightarrow n_s \text{ mod } 2 = 0$
  $Z_2 = (n_0^{M,-} + n_\pi^{M,-}) \text{ mod } 2 = 1$
  $\rightarrow n_s \text{ mod } 2 = 1$

Jun-Won Rhim, Jan Behrends, Jens H. Bardarson, Phys. Rev. B 95, 035421 (2017).

AGNR

- $Z_2 = \frac{1-(-1)^{[\frac{4}{3}]+[\frac{4+1}{2}]}}{2} = 1$

N	$n_0^{M,-}$	$n_\pi^{M,-}$	$Z_2 = n_0^{M,-} + n_\pi^{M,-} \bmod 2$	n_s
4	1	2	1	1

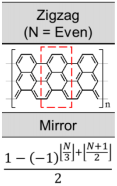

Figure 3: Zigzag

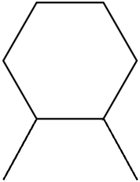

Figure 4: N=4

Ting Cao, Fangzhou Zhao, and Steven G. Louie, Phys. Rev. Lett. 119, 076401 (2017).

AGNR

- $Z_2 = \frac{1-(-1)^{[\frac{7}{3}]+[\frac{7+1}{2}]}}{2} = 0$

N	$n_0^{I,-}$	$n_\pi^{I,-}$	$Z_2 = n_0^{I,-} + n_\pi^{I,-} \bmod 2$	n_s
7	3	3	0	0
N	$n_0^{M,-}$	$n_\pi^{M,-}$	$Z_2 = n_0^{M,-} + n_\pi^{M,-} \bmod 2$	n_s
7	2	4	0	0

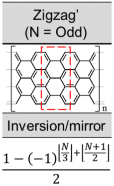

Figure 5: Zigzag'

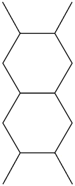

Figure 6: N=7

Chevron-type GNRs

- "Graphene nanoribbons, or single-layer graphite are predicted to exhibit electronic properties that make them attractive for the fabrication of nanoscale electronic devices."

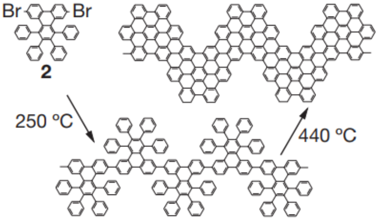

Atomically precise bottom-up fabrication of graphene nanoribbons, Nature 466, 470–473 (2010).

Chevron-type GNRs

- Mirror symmetry
- $Z_2 = 1$

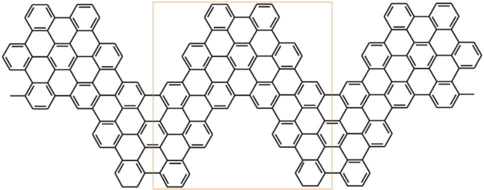

Figure 7: Mirror symmetry

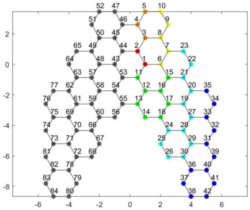

Figure 8: Unit cell

Atomically precise bottom-up fabrication of graphene nanoribbons, Nature 466, 470–473 (2010).

Chevron-type GNRs

- Inversion symmetry
- $Z_2 = 0$

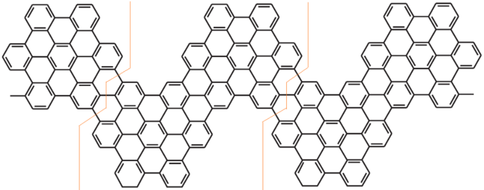

Figure 9: Inversion symmetry

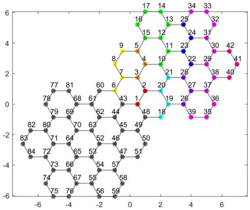

Figure 10: Unit cell

Atomically precise bottom-up fabrication of graphene nanoribbons, Nature 466, 470–473 (2010).

Chevron-type GNRs

- Check band structure
- Band structure calculated by DFT
- Band structure calculated by TB

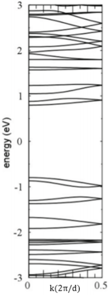

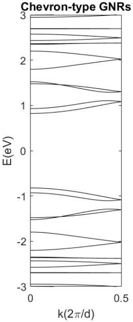

Atomically precise bottom-up fabrication of graphene nanoribbons, Nature 466, 470–473 (2010).

Chevron-type GNRs

- Mirror symmetry
  $Z_2 = 1 \rightarrow n_s \bmod 2 = 1$
  Surface state: 1 pair
- Inversion symmetry
  $Z_2 = 0 \rightarrow n_s \bmod 2 = 0$
  Surface state: 0 pair

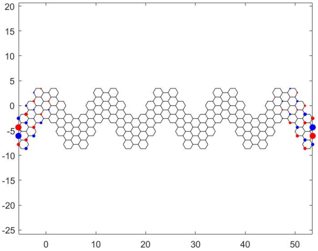

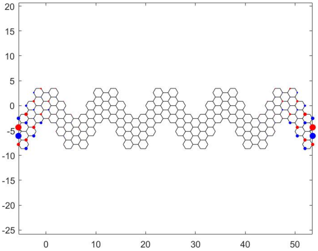

Chevron-type GNRs

1.74636310509769e-07

-1.74636310509769e-07

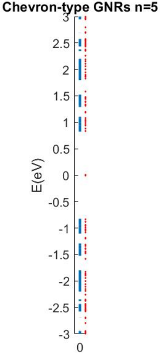

Figure 11: Mirror symmetry

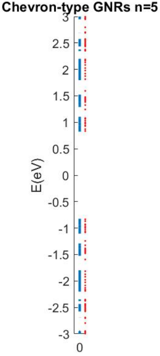

Figure 12: Inversion symmetry

Summary

- Bulk: Z_2 (Zak phase)
  Edge: Surface states (Edge states)
  Bulk Edge correpondence: Z_2 predicts n_s
- In chevron-type GNRs,
  Z_2 depends on the end termination.
- In chevron-type GNRs,
  Z_2 successfully predicts the number of surface states.
- Future work:
  Combine the 2 types of unit cell might show surface states.

The End

Appendix-1 Tight-binding Model

- Tight-binding approximation
  $$H = \sum_i \epsilon_i \left|i\right\rangle \left\langle i\right| - \sum_{i,j} t_{i,j} \left|i\right\rangle \left\langle j\right|$$
  on-site term - hopping term
- Schrödinger's equation
  $$H\Psi = E\Psi$$
  $$\begin{pmatrix} \epsilon & \mu \\ \mu^* & \epsilon \end{pmatrix} \begin{pmatrix} C_A \\ C_B \end{pmatrix} = E \begin{pmatrix} C_A \\ C_B \end{pmatrix}$$

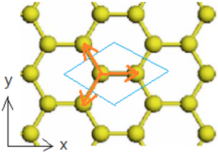

Huaixiu Zheng, Z. F. Wang, Tao Luo, Q. W. Shi, and Jie Chen, Phys. Rev. B 75, 165414, (2007).

Appendix-1 Tight-binding Model

- Bloch's theorem

$$|\Psi\rangle_A = \frac{1}{N_A} \sum_{i=1}^{N} \sum_{x_{A_i}} e^{ik_x x_{A_i}} \phi_A(i) \, |A_i\rangle$$

$$|\Psi\rangle_B = \frac{1}{N_B} \sum_{i=1}^{N} \sum_{x_{B_i}} e^{ik_x x_{B_i}} \phi_B(i) \, |B_i\rangle$$

- Boundary Condition

$\phi_A(0) = \phi_B(0) = 0$

$\phi_B(N+1) = \phi_B(N+1) = 0$

N: width of the unit cell

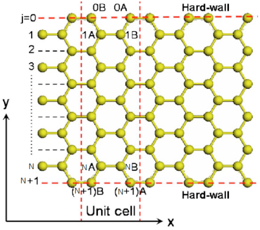

Huaixiu Zheng,Z. F. Wang, Tao Luo, Q. W. Shi, and Jie Chen, Phys. Rev. B 75, 165414 (2007).

Appendix-1 Tight-binding Model

- BC solution
  $\phi_A(i) = \phi_B(i) = \sin\left(\frac{\sqrt{3}a}{2} q_y\right) = 0$
  $q_y = \frac{2}{\sqrt{3}a} \frac{p\pi}{N+1}$
  $p = 1, 2, ..., n$(band pair number)
- $\mu =_A \langle \Psi | H | \Psi \rangle_B = -t[2e^{-ik_x a/2} \cos\left(\frac{\sqrt{3}a}{2} q_y\right) + e^{ik_x a}]$
- $E = \epsilon \pm |\mu|$, $\epsilon = 0$
  $E = \pm t |2e^{-ik_x a/2} \cos\left(\frac{\sqrt{3}a}{2} q_y\right) + e^{ik_x a}|$

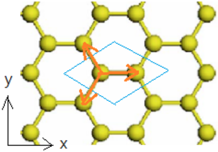

$$\delta_1 = (a, 0)$$
$$\delta_2 = \left(-\frac{a}{2}, \frac{\sqrt{3}a}{2}\right)$$
$$\delta_3 = \left(-\frac{a}{2}, -\frac{\sqrt{3}a}{2}\right)$$

Huaixiu Zheng,Z. F. Wang, Tao Luo, Q. W. Shi, and Jie Chen, Phys. Rev. B 75, 165414 (2007).

Appendix-2 ZGNR Edge State

- Bloch's theorem→Boundary:e^{ikn}
  Fermi level→A solution of $E = 0$
  Charge density $\propto \cos^{-2m}(\frac{k}{2})$

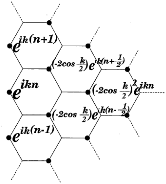

Figure 13: Analytical scheme of wave functions

Appendix-3 Zak Phase and Wave Parity

- Bloch Hamiltonian
  $H(k)\left|u_{nk}\right\rangle = E_{nk}\left|u_{nk}\right\rangle$
- Inversion symmetry
  $IHI^{-1} = H$
  $IH(k)I^{-1} = H(-k)$
- Phase relation
  $I\left|u_{nk}\right\rangle = e^{i\phi(k)}\left|u_{n-k}\right\rangle$
- Zak phase
  $Z = \int_{-\pi}^{\pi} dki\left\langle u_{nk}\middle|\partial_k\middle|u_{nk}\right\rangle$

Appendix-3 Zak Phase and Wave Parity

- Calculated result by using the above material
  $Z = -\int_0^{\pi} dk \frac{\partial \phi(k)}{\partial k} = \phi(0) - \phi(\pi)$
- $H(\pi)\,|u_{n\pi}\rangle = E_{n\pi}\,|u_{n\pi}\rangle$
  $I\,|u_{n\pi}\rangle = \xi_n(\pi)\,|u_{n\pi}\rangle$,$\xi_n(\pi) = e^{i\phi(\pi)}$
  $H(0)\,|u_{n0}\rangle = E_{n0}\,|u_{n0}\rangle$
  $I\,|u_{n0}\rangle = \xi_n(0)\,|u_{n0}\rangle$,$\xi_n(0) = e^{i\phi(0)}$
- $e^{i(\phi(0)-\phi(\pi))} = \xi_n(0)/\xi_n(\pi) = \xi_n(0)\xi_n(\pi)$
- $(-1)^{Z_2} = e^{i\sum\limits_n \gamma_n^{inter}} = \prod\limits_{k=0,\pi} \delta(k)$
  $\delta(k) = \prod\limits_{n \in occupied} \xi_n(k)$